THE JOURNAL OF PHYSICAL CHEMISTRY LETTERS
A JOURNAL OF THE AMERICAN CHEMICAL SOCIETY

pubs.acs.org/JPCL

Letter

Crossed Beam Experiments and Computational Studies of Pathways to the Preparation of Singlet Ethynylsilylene (HCCSiH; X^1A'): The Silacarbene Counterpart of Triplet Propargylene (HCCCH; X^3B)

Adam Rettig, Martin Head-Gordon,* Srinivas Doddipatla, Zhenghai Yang, and Ralf I. Kaiser*

Cite This: *J. Phys. Chem. Lett.* 2021, 12, 10768−10776

Read Online

ACCESS | Metrics & More | Article Recommendations | Supporting Information

ABSTRACT: Ethynylsilylene (HCCSiH; X^1A') has been prepared in the gas phase through the elementary reaction of singlet dicarbon (C_2) with silane (SiH_4) under single-collision conditions. Electronic structure calculations reveal a barrierless reaction pathway involving 1,1-insertion of dicarbon into one of the silicon−hydrogen bonds followed by hydrogen migration to form the 3-sila-methylacetylene ($HCCSiH_3$) intermediate. The intermediate undergoes unimolecular decomposition through molecular hydrogen loss to ethynylsilylene (HCCSiH; C_s; X^1A'). The dicarbon−silane system defines a benchmark to explore the consequence of a single collision between the simplest "only carbon" molecule (dicarbon) with the prototype of a closed-shell silicon hydride (silane) yielding a nonclassical silacarbene, whose molecular geometry and electronic structure are quite distinct from the isovalent triplet propargylene (HCCCH; C_2; ^3B) carbon-counterpart. These organosilicon transients cannot be prepared through traditional organic, synthetic methods, thus opening up a versatile path to access the previously largely elusive class of silacarbenes.

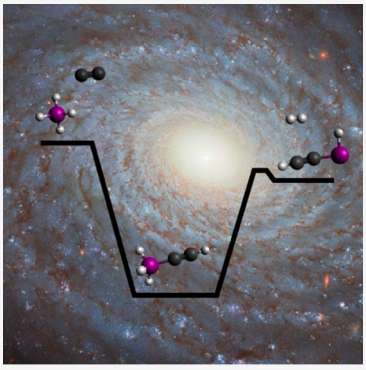

Since the groundbreaking detection of cyclopropenylidene (c-C_3H_2, X^1A_1, **1**), vinylidenecarbene (H_2CCC, X^1A_1, **2**), and propargylene (HCCCH, X^3B, **3**) in the laboratory and in interstellar and circumstellar environments,[1] isomers of C_3H_2 (**1**−**3**) and their isovalent SiC_2H_2 species (**p1**−**p6**) have attracted substantial interest from the physical (organic) and computational chemistry communities from the fundamental points of view of chemical bonding and electronic structure theory (Scheme 1). Singlet cyclopropenylidene (c-C_3H_2; **1**; C_{2v}; $^1A_1$) represents the global minimum of the C_3H_2 surface; this isomer can be best described as a highly unsaturated (partially) 2π-Hückel aromatic, C_{2v} symmetric three membered ring molecule with an apical carbene carbon. Cyclopropenylidene was first detected by Reisenauer et al. in low-temperature argon matrices at 10 K[1] prior to its identification in a helium−acetylene gas discharge[2] and toward the Taurus Molecular Clouds (TMC-1). Photon exposure at 313 nm converts cyclopropenylidene (c-C_3H_2; **1**; C_{2v}; $^1A_1$) to triplet propargylene (HCCCH; **3**; C_2; ^3B), which itself isomerizes to singlet vinylidenecarbene (H_2CCC; **2**; C_{2v}; $^1A_1$).[3] The latter was identified in a helium−acetylene discharge prior to its observation toward TMC-1.[4] The C_2 symmetric triplet propargylene (HCCCH; **3**; C_2; ^3B) has each unpaired electron formally localized at each terminal carbon atom.[5,6] This results in a 1,3-diradical, which is at least 53 kJ mol^{-1} more stable than its a^1A' singlet state.[7] Crossed molecular beam studies revealed that cyclopropenylidene (**1**) together with vinylidenecarbene (**2**) and/or propargylene (**3**) can be prepared through elementary gas-phase reactions of methylidyne ($CH(X^2\Pi)$) with acetylene ($C_2H_2(X^1\Sigma_g^+)$)[8] and of ground-state carbon atoms ($C(^3P)$) with the vinyl radical ($C_2H_3(X^2A')$).[9]

The substitution of a single carbon atom by an isovalent silicon atom leads to SiC_2H_2 isomers (**p1**−**p6**). In analogy to the isovalent cyclopropenylidene (c-C_3H_2, X^1A_1, **1**), singlet 1-silacyclopropenylidene (c-SiC_2H_2; **p1**; C_{2v}; $^1A_1$) represents the global minimum on the SiC_2H_2 surface.[10] Maier et al. generated **4** by pulsed flash pyrolysis of 2-ethynyl-1,1,1-trimethyldisilane and trapping in argon matrix at 10 K.[11] These authors also revealed that co-condensation of atomic silicon and acetylene in an argon matrix leads to addition of silicon to the carbon−carbon triple bond and—after inter system crossing (ISC)—to 1-silacyclopropenylidene (c-SiC_2H_2; **p1**; C_{2v}; $^1A_1$).[12] Izuha et al. recorded the rotational spectrum of **p1** after discharging a mixture of silane (SiH_4), acetylene (C_2H_2), and helium.[13] Photolysis of **p1** in an argon matrix leads to the higher energy isomers ethynylsilylene (HCCSiH; **p3**; C_s; $^1A'$), vinylidenesilanediyl ($SiCCH_2$; **p2**; C_{2v}; $^1A_1$), and silacyclopropyne (c-$CCSiH_2$; **p5**; C_{2v}; $^1A_1$).[11] Among these higher-energy isomers, only singlet vinylidenesilanediyl ($SiCCH_2$; **p2**; C_{2v}; $^1A_1$) was characterized via Fourier transform microwave

Received: September 14, 2021
Accepted: October 8, 2021

Scheme 1. Molecular Structures, Electronic Ground State Wave Functions, Point Groups, and the Relative Energies of C_3H_2 (1−3) and SiC_2H_2 (p1−p6) Isomers[a]

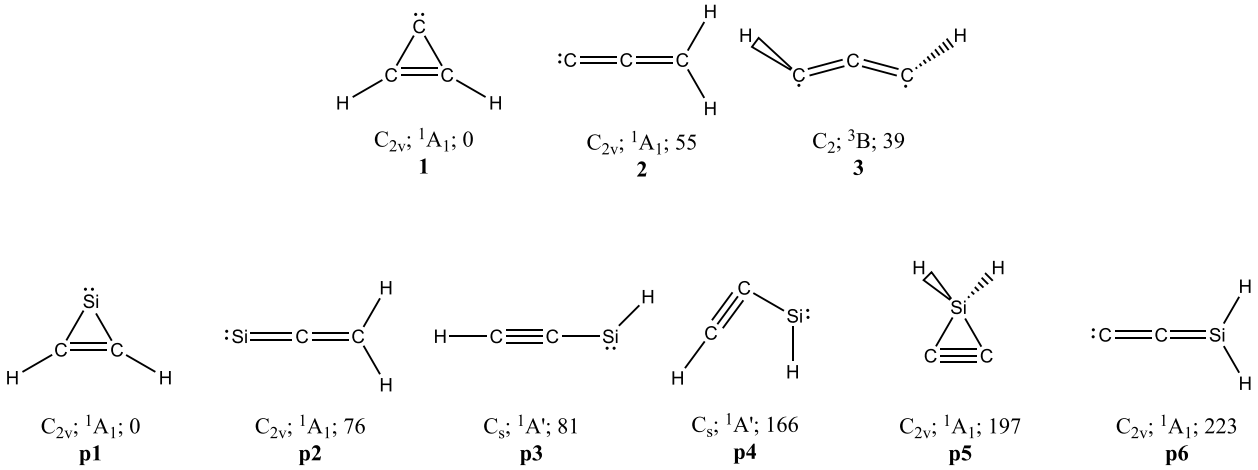

[a]Energies are shown in kJ mol^{-1}.

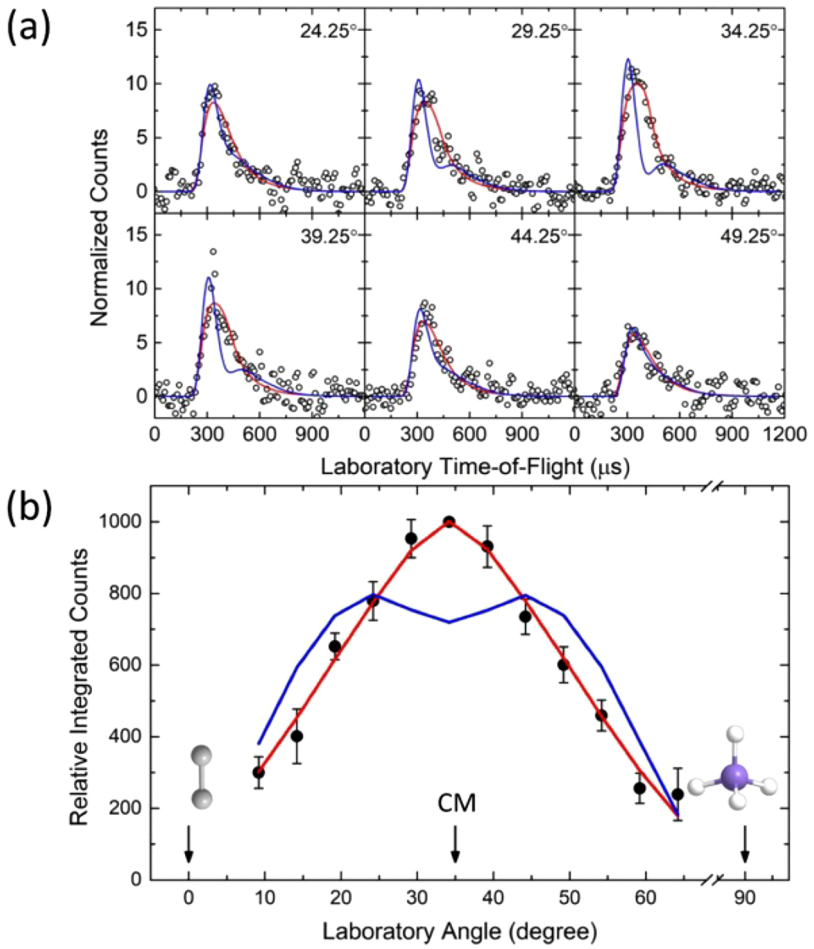

Figure 1. (a) Time-of-flight (TOF) spectra recorded at m/z = 54 ($C_2SiH_2^+$) for reaction of dicarbon (C_2; $X^1\Sigma_g^+/a^3\Pi_u$) with silane (SiH_4; X^1A_1). The open circles are experimental data; the quasiclassical theory (QCT)-based fit is shown in blue, and the fit resulting from the "best fit" center-of-mass translational energy distribution is shown in red. (b) Laboratory angular distribution obtained at m/z = 54 ($C_2SiH_2^+$) from the reaction of dicarbon (C_2;$X^1\Sigma_g^+/a^3\Pi_u$) with silane (SiH_4; X^1A_1). The circles are experimental data; the QCT-based fit is shown in blue, and the fit resulting from the "best fit" center-of-mass translational energy distribution is shown in red.

spectroscopy.[14] It is important to note that the carbon analogue of **p5**—the singlet cyclopropyne molecule c-$CCCH_2$ (X^1A_1)—is a saddle point; triplet cyclopropyne (a^3B_2), however, was found to be a local minimum.[15] This reveals that a replacement of a single carbon by an isovalent silicon atom leads to molecules such as silacyclopropyne (c-

https://doi.org/10.1021/acs.jpclett.1c03036
J. Phys. Chem. Lett. 2021, 12, 10768−10776

$CCSiH_2$; **p5**; C_{2v}; $^1A_1$), whose carbon analogue does not exist.[11] Considering the complexity of a *directed* gas-phase synthesis under single-collision conditions, which so far has led only to the preparation of silacyclopropenylidene (c-SiC_2H_2; **p1**; C_{2v}; $^1A_1$),[16] and the short lifetimes of these transient species under "bulk" conditions, free silacarbenes 1-silacyclopropenylidene (**p1**), vinylidenesilanediyl (**p2**), ethynylsilylene (**p3**), ethynylisilylene (**p4**), silacyclopropyne (**p5**), and silavinylidenecarbene (**p6**) exemplify one of the most obscured classes of organic transient molecules.

Herein, we present a peek into the unknown gas-phase chemistry of ethynylsilylene (HCCSiH; **p3**; C_s; $^1A'$), the isovalent counterpart of triplet propargylene (HCCCH; **3**; C_2; ^3B). This is achieved by preparing ethynylsilylene under single-collision conditions via the bimolecular reaction of singlet dicarbon (C_2) with silane (SiH_4) employing the crossed molecular beams method and merging the experiments with electronic structure calculations and dynamics simulations. An investigation at the most fundamental, microscopic level reveals new insights into the reaction mechanisms and inherent chemical dynamics through which highly reactive organosilicon molecules such as ethynylsilylene (HCCSiH; **p3**) are synthesized in the gas phase. Besides the physical organic chemistry viewpoint of understanding structure, reactivity, and bond-breaking processes, the dicarbon−silane system is also attractive from the astrophysical viewpoint to elucidate fundamental reaction pathways to silacarbenes, which so far have eluded detection in interstellar and carbon-rich circumstellar environments although the dicarbon and silane reactants are omnipresent in carbon-rich envelopes such as of the carbon-star IRC+10216. Our approach reveals previously obscure gas-phase chemistry that directly accesses a fascinating class of highly unsaturated silacarbenes under controlled conditions: ethynylsilylene (HCCSiH; **p3**).

The crossed molecular beams studies were carried out at a collision energy of 22.0 ± 0.3 kJ mol^{-1}.[17] Dicarbon was produced by photodissociation of tetrachloroethylene (C_2Cl_4, Sigma-Aldrich, 99.9%) at 248 nm seeded in helium (99.9999%; AirGas) at levels of 1.4% at 300 K.[18] Singlet and triplet C_2 was detected by laser-induced fluorescence.[19] The supersonic beam of dicarbon (C_2; $X^1\Sigma^+_g/a^3\Pi_u$; 24 amu) crossed a beam of silane (SiH_4; X^1A_1; 32 amu) perpendicularly in the interaction region of the scattering chamber (Methods; Table S1). A triply differentially pumped quadrupole mass spectrometer (QMS) operated at 10^{-11} Torr in conjunction with an electron impact ionizer (80 eV; 2 mA) was then exploited to record time-of-flight spectra (TOF) and the product angular distribution of the reactively scattered products in the scattering plane at mass to charge ratios (m/z) from m/z = 56 ($C_2H_4Si^+$) to 52 (C_2Si^+). It should be noted that the TOF mode does not record a traditional mass spectrum; the TOF mode records the flight time of the neutral molecule from the collision center to the detector, after ionization of the neutral product, at a well-defined mass-to-charge (m/z) ratio. TOF spectra at different m/z ratios can be collected by selecting a particular m/z ratio using the QMS and recording the TOF for each m/z setting independently.[15]

Reactive scattering signal was detected from m/z = 54 to 52; after scaling, the TOF spectra recorded from m/z = 54 to 52 were superimposable. The scattering signal decreased from m/z = 54 via m/z = 53 to m/z = 52. Reactive scattering signal was therefore collected at m/z = 54 ($C_2H_2{}^{28}Si^+$) (Figure 1), but not at m/z = 53 and 52, which result from dissociative electron impact ionization of the neutral parent. These data propose the existence of a single reaction channel leading to $C_2H_2{}^{28}Si$ isomer(s) (54 amu) (hereafter: C_2H_2Si) along with molecular hydrogen (2 amu). Neither adducts ($C_2H_4{}^{28}Si$; 56 amu) nor the atomic hydrogen loss pathway forming C_2H_3Si isomer(s) (55 amu) were observable. Accounting for the signal at m/z = 54 and for the natural isotope abundances of silicon of ^{30}Si(3.1%), ^{29}Si(4.67%), and ^{28}Si(92.23%), the signal for m/z = 55 ($C_2H_2{}^{29}Si^+$) and m/z = 56 ($C_2H_2{}^{30}Si^+$) is below the detection limit. The laboratory angular distribution is very broad and spread over at least 55° in the scattering plane, indicating a substantial energy release into the translational degrees of freedom of the products. Furthermore, the nearly forward−backward symmetry of the laboratory angular distribution implies indirect scattering dynamics involving metastable C_2H_4Si collision complex(es).

To obtain fundamental information on the underlying reaction mechanisms leading to C_2H_2Si isomer(s), the laboratory data were fit with a forward-convolution routine eventually providing an angular flux distribution, $T(\theta)$, and a translational-energy flux distribution, $P(E_T)$, in the center-of-mass reference frame (Figure 2). The laboratory data could be

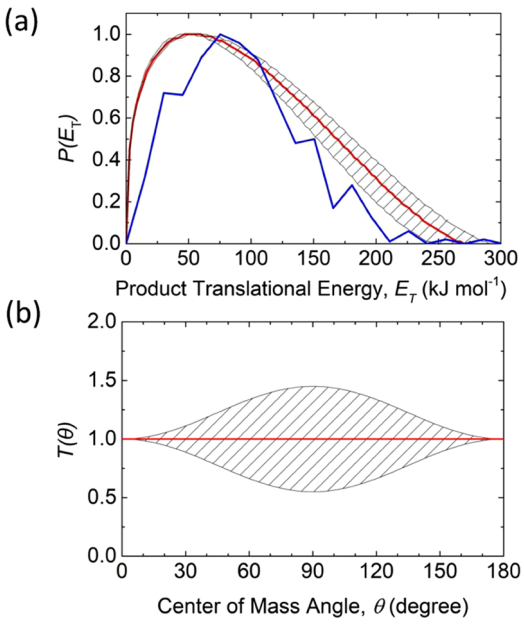

Figure 2. Center-of-mass translational energy (a) and angular (b) flux distributions for the formation of C_2SiH_2 isomers plus molecular hydrogen via the reaction of dicarbon (C_2; $X^1\Sigma^+_g/a^3\Pi_u$) with silane (SiH_4; X^1A_1). The hatched areas define regions of acceptable fits. In panel a, the center-of-mass translational energy distribution obtained by QCT calculations is provided in blue.

replicated with a single-channel fit leading to the formation of C_2H_2Si (54 amu) isomers plus molecular hydrogen (2 amu). The center-of-mass translational energy distribution, $P(E_T)$, displays a high-energy cutoff of 270 ± 20 kJ mol^{-1}. Under favorable circumstances, for molecules formed without internal excitation, the high-energy cutoff is the sum of the reaction exoergicity plus the collision energy. In this limit, a subtraction of the collision energy would suggest that the reaction is exoergic by 248 ± 20 kJ mol^{-1}. Further, the $P(E_T)$ peaks away from zero translational energy, revealing a broad plateau from 30 to 70 kJ mol^{-1}; this finding would be consistent with a tight

https://doi.org/10.1021/acs.jpclett.1c03036
J. Phys. Chem. Lett. 2021, 12, 10768−10776

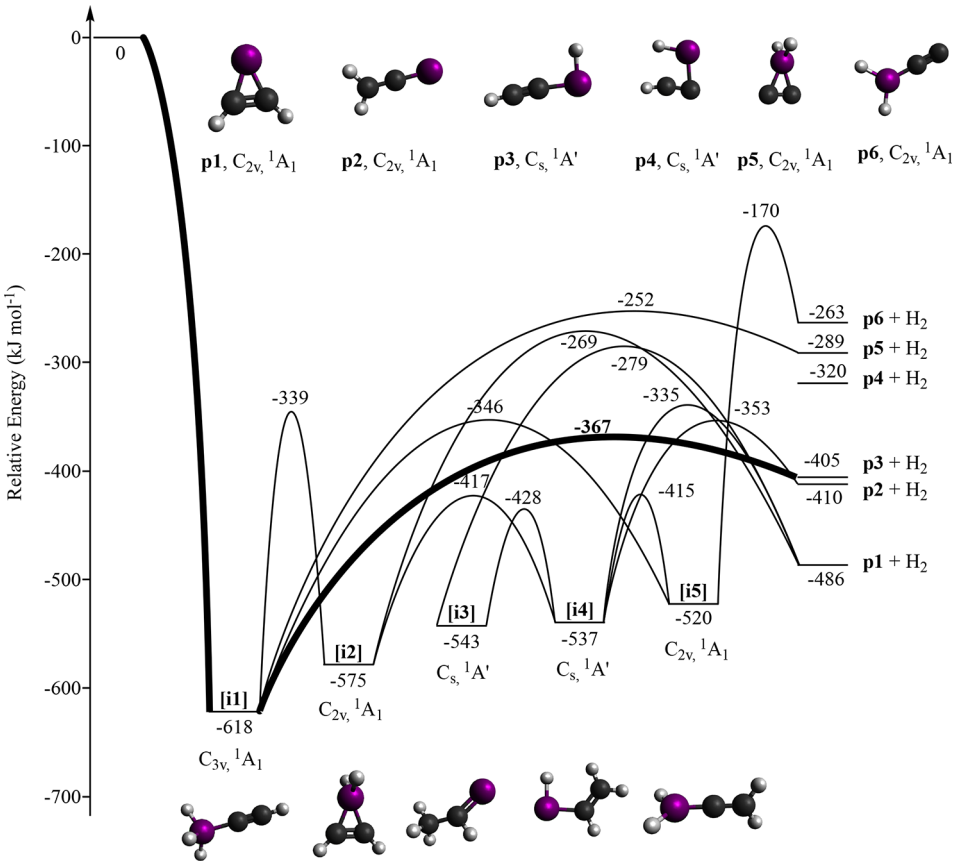

Figure 3. Potential energy surfaces (PESs) (in kJ mol^{-1}) for the reactions of singlet dicarbon with silane along with electronic ground-state symmetries and point groups of intermediates and products. The lowest-energy pathway from reactants to products is in bold. Atoms are color coded in white (hydrogen), purple (silicon), and black (carbon). Structures and vibrational frequencies are provided for the reactants, intermediates, transition states, and products in the Supporting Information (Table S2).

exit transition state and hence significant electron reorganization upon decomposition of the C_2H_4Si intermediate(s) upon molecular hydrogen loss. In addition, the center-of-mass angular distribution, $T(\theta)$, exhibits flux over the complete angular range from 0° to 180°. This finding is indicative of indirect (complex forming) dynamics involving C_2H_4Si intermediate(s), whose lifetime(s) is/are longer than the(ir) rotational period(s).

For complex poly atomic systems, it is beneficial to combine crossed molecular beam studies with electronic structure calculations (Figure 3). These calculations (Methods) predict the overall reaction energies and barriers to an accuracy of about 5 kJ mol^{-1}.[20] Our computations revealed the existence of six C_2H_2Si isomers (**p1**−**p6**) formed in reactions that are overall exoergic by between 486 ± 5 and 263 ± 5 kJ mol^{-1}. The relative stabilities of these isomers correlate well with previous computational studies by Mebel et al., Ghambarian et al., Talbi, Schaefer et al., and Thorwirth et al.[21−26] Our computations suggest that for singlet dicarbon, the reaction is initiated by a defacto barrierless insertion of the singlet dicarbon molecule into one of the four silicon−hydrogen bonds of silane leading to singlet 3-sila-methylacetylene ($HCCSiH_3$; [**i1**]) (Figure 4). This C_{3v} symmetric intermediate is the global minimum on the singlet C_2H_4Si potential energy surface. The pathway from the reactants to 3-sila-methylacetylene ($HCCSiH_3$; [**i1**]) is downhill by more than 600 kJ mol^{-1} and overall barrierless. Two mechanisms to reach this intermediate, potentially depending on the starting configuration, seem possible. First, as observed in both ab initio dynamics trajectories and geometry optimizations, 1,1-dicarbon insertion occurs into one of the four chemically equivalent Si−H bonds in conjunction with rapid hydrogen migration (Figure 4a). Second, some trajectories also show initial hydrogen abstraction, yielding an ethynyl radical (CCH) and a silyl radical (SiH_3) immediately followed by recombination of the radical fragments to ($HCCSiH_3$; [**i1**]) (Figure 4b); this pathway suggests the possibility of a roaming mechanism. Starting from [**i1**], multiple isomerization pathways access sila-cyclopropene (c-C_2SiH_4; [**i2**]), 1-sila-2-methylvinylidene ($SiCH(CH_3)$; [**i3**]), 3-sila-vinylcarbene (C_2H_3SiH; [**i4**]), and 1-sila-allene (H_2CCSiH_2; [**i5**]) involving hydrogen shifts along with ring closure/opening through transition states located well below the energy of the separated reactants. The computations also reveal eight unimolecular decomposition pathways to the reaction products (**p1**−**p6**) with overall tight exit transition states located between 38 and 93 kJmol^{-1} above the initially formed products. While no pathway to **p4** was found from the intermediates, **p4** can be accessed in principle via isomerization of **p3** and/or **p5** (Figure S2). On the triplet surface, our computations show that the most stable C_2H_4Si intermediates are over 150 kJ mol^{-1} higher in energy than [**i5**]; the reactions will therefore cross over to the singlet surface if possible. The singlet−triplet gap during a typical ab initio trajectory of the silane−triplet dicarbon reaction becomes negligible as the dicarbon molecule nears silane, providing an avenue for the triplet reactants to cross

https://doi.org/10.1021/acs.jpclett.1c03036
J. Phys. Chem. Lett. 2021, 12, 10768−10776

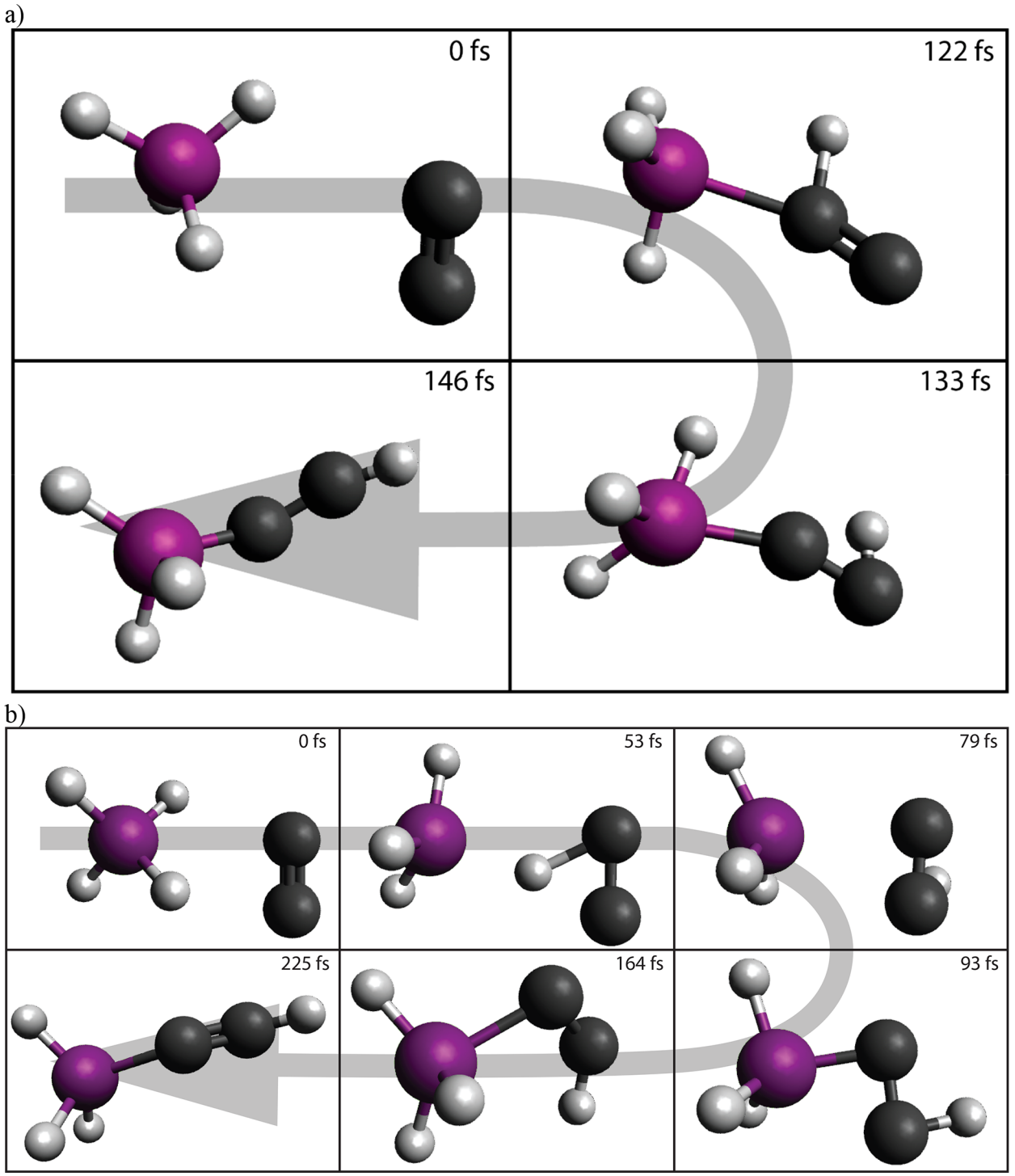

Figure 4. Snapshots along the reaction coordinate for (a) an initial barrierless 1,1-insertion of singlet dicarbon into a silicon−hydrogen bond of silane followed by hydrogen migration leading to the 3-sila-methylacetylene ($HCCSiH_3$) intermediate [i1] and (b) a hydrogen abstraction leading to the ethynyl and silyl radical pair followed by radical−radical recombination to 3-sila-methylacetylene ($HCCSiH_3$) intermediate [i1].

over to the singlet surface via spin−orbit coupling. Only singlet intermediates are therefore predicted.

Under normal circumstances, a comparison of the experimentally derived reaction energy of 248 ± 20 kJ mol^{-1} with the computed reaction energies leading to the products **p1**−**p6** would reveal the nature of the (dominant) reaction channel. In the present situation, however, the present reaction is more complex. Based on the experimental findings, this procedure would suggest the formation of silavinylidenecarbene (H_2SiCC; **p6**; X^1A_1). This product can be accessed via unimolecular decomposition of 1-sila-allene (H_2CCSiH_2; [**i5**]), which in turn is accessible from singlet 3-sila-methylacetylene ($HCCSiH_3$; [**i1**]) via hydrogen migration (pathway 1) and also through the isomerization sequence [**i1**] → [**i2**] → [**i4**] → [**i5**] (pathway 2). However, considering the energies of the transition states for pathways 1 and 2 of 174 kJ mol^{-1} and up to 236 kJ mol^{-1}, respectively, the unimolecular decomposition of 3-sila-methylacetylene ($HCCSiH_3$; [**i1**]) to

https://doi.org/10.1021/acs.jpclett.1c03036
J. Phys. Chem. Lett. 2021, 12, 10768−10776

ethynylsilylene (HCCSiH; **p3**) via an exit transition state located only 38 kJ mol^{-1} above the final products should be preferred. Because all four hydrogen atoms in silane are chemically equivalent, it is not feasible to conduct crossed beam experiments with partially deuterated reactants to trace the lost hydrogen(s) and/or deuterium(s).[27] One possible explanation to converge the aforementioned finding is that ethynylsilylene (HCCSiH; **p3**) does form in the crossed beam reaction, but the products are highly internally (rovibrationally) excited so that less than the experimentally derived reaction energy is released into the translational degrees of freedom of the final products. This in turn would result in a $P(E_T)$ with a lower maximum translational energy than expected based on the computational predictions. The products can further isomerize because of an abundance of rovibrational energy and relatively low barriers between products; this of course will not affect the product translational energy however.

To test this hypothesis, we conducted Rice−Ramsperger−Kassel−Marcus (RRKM) calculations and carried out quasiclassical trajectory calculations (QCT) (Methods). RRKM theory assumes complete randomization of the available energy. Starting from the initial collision complex 3-sila-methylacetylene ($HCCSiH_3$; [**i1**]), the RRKM treatment at a collision energy of 22 kJmol^{-1} predicts a predominant formation of ethynylsilylene (HCCSiH; **p3**; 90%) and vinylidenesilanediyl ($SiCCH_2$; **p2**; 8%) with only minor contributions of the remaining isomers of 2% (Supporting Information). These initially formed products can further isomerize; however, RRKM theory predicts that substantial fractions of **p3** exceeding 55% will remain after 1 ns even with the maximum possible product internal energy (Supporting Information). Hereafter, quasiclassical trajectory (QCT) calculations were carried out (Methods; Supporting Information). These calculations bridge the dynamics experiments and the theoretical understanding of the reaction and also provide theoretically predicted center-of-mass translational energy distributions ($P(E_T)$) (Figure 2); these predicted distributions can be exploited then to fit the experimental data (Figure 1). The QCT calculations were launched from the transition states, as the hot intermediates are too long-lived to study on a reasonable QCT time scale; trajectories run for 2.5 ps from the hot intermediates showed no reaction. The dynamics studies leading to ethynylsilylene (HCCSiH; **p3**) predict a center-of-mass translational energy distribution with a high-energy cutoff of 250 ± 20 kJ mol^{-1}. Within the error limits, this data correlates nicely with the best fit center-of-mass functions based on our experimental data of 270 ± 20 kJ mol^{-1} (Figure 2). Therefore, we can conclude that the QCT treatment of the trajectories to ethynylsilylene (HCCSiH; **p3**) suggests that ethynylsilylene (HCCSiH; **p3**) is formed highly rovibrationally excited. This internal energy in turn results in a $P(E_T)$ with a maximum translational energy well below the computed reaction energy of 405 ± 5 kJ mol^{-1}. Nevertheless, the distribution maximum of the predicted $P(E_T)$ is shifted by about 25 kJ mol^{-1} to higher energies. This might be caused by leakage of zero-point energy (explicitly considered in quasiclassical dynamics) into other modes, leading to greater peak translational energies of the products than expected. Essentially, this shift results in simulated TOF spectra which are slightly faster than recorded experimentally; likewise, this excess energy is reflected in a much broader laboratory angular distribution than determined experimentally (Figure 1). Nevertheless, despite this open issue, RRKM studies, QCT calculations, and the experiments can be reconciled with the formation of highly rovibrationally excited ethynylsilylene (HCCSiH; **p3**) along with molecular hydrogen in an overall exoergic and entrance barrierless bimolecular reaction.

From the viewpoint of electronic structure and chemical bonding, it is educational to compare singlet ethynylsilylene (HCCSiH; X^1A') with triplet propargylene (HCCCH; X^3B) (Scheme 2). The replacement of a carbon atom by an isovalent

Scheme 2. Molecular Structures of Triplet Propargylene (HCCCH; X^3B) Computed by Stanton and McMahon et al.[31] and Singlet Ethynylsilylene (HCCSiH; X^1A') Computed via DFT (Methods)[a]

[a]Bond angles are presented in degrees, and bond lengths are provided in Angstroms.

silicon atom first changes the geometry from C_2 to C_s and the multiplicity from a triplet to a singlet. This dramatic switch can be best rationalized by defining triplet propargylene as a 1,3-diradical with parallel spin, but with singlet ethynylsilylene as a silacarbene with both electrons paired and localized at the silicon atom. This agrees with previous theoretical studies showing silicon tends to avoid multiple bonds, instead preferring to localize nonbonding electrons onto the silicon atom.[28] This is clearly seen through the geometries of propargylene and ethynylsilyene. Propargylene has two C−C bonds with length 1.27 Å—somewhere between the length of a typical double and triple bond; the substitution of one carbon for a silicon in ethynylsilylene leads to a Si−C bond length of 1.84 Å, more consistent with a single bond. The H−Si−C bond angle of 93.2° in ethynylsilylene compared to 162.0° in propargylene shows that the lone pair on the silicon resides in an atomic orbital with a large amount of s character while the unpaired electrons in propargylene reside in p orbitals; this is consistent with previous studies of silicon-containing compounds, where the behavior is attributed to the inert pair effect.[28−30]

To conclude, our study utilizing crossed molecular beam experiments combined with statistical and quasi classical trajectory analysis of the gas-phase reaction of singlet and triplet dicarbon with silane affords persuasive evidence for the very first directed gas-phase preparation of the C_s symmetric singlet ethynylsilylene (HCCSiH; **p3**; $^1A'$). The reaction of singlet dicarbon is initiated by a barrierless insertion of dicarbon into the silicon−hydrogen bond of silane leading effectively via 1,2-insertion to the singlet 3-sila-methylacetylene ($HCCSiH_3$; [**i1**]) collision complex. Alternatively, dicarbon may abstract a hydrogen yielding an ethynyl radical (CCH) and a silyl radical (SiH_3) followed by either rapid recombination or possibly a delayed roaming mediated reaction of the radical fragments to 3-sila-methylacetylene. Triplet dicarbon ends up at the same intermediate through spin−orbit coupling between the triplet and singlet surfaces. This intermediate then undergoes predominantly unimolecular decomposition via molecular hydrogen loss to highly rovibrationally excited singlet ethynylsilylene (HCCSiH; **p3**; $^1A'$). The initial insertion of dicarbon to form a bound 3-sila-

https://doi.org/10.1021/acs.jpclett.1c03036
J. Phys. Chem. Lett. 2021, 12, 10768−10776

methylacetylene ($HCCSiH_3$; [**i1**]) intermediate essentially bypasses the traditionally "expected" route via singlet silylcarbene ($CCH(SiH_3)$) through 1,1-insertion, which was revealed not to be a local minimum. This insertion process is in strong contrast to the isovalent dicarbon−methane system, in which dicarbon inserts through 1,1-insertion with only one carbon atom yielding a bound singlet methylcarbene ($CCH-(CH_3)$) intermediate, which reacts via hydrogen migration to singlet methylacetylene ($HCCCH_3$; X^1A_1).[32] This defines the dicarbon−silane system as a prototype of a novel, exotic insertion mechanism through carbon−silicon bond formation eventually leading to highly unsaturated singlet ethynylsilylene (HCCSiH; **p3**; $^1A'$), thus clarifying our understanding of reactivity, molecular structure, and the dynamics of silicon-containing reaction mechanisms. The facile preparation and identification of gas-phase singlet ethynylsilylene (HCCSiH; **p3**; $^1A'$) also has significant implications for the chemistry in circumstellar environments of carbon-rich asymptotic giant branch (AGB) stars such as IRC+10216. The astronomical detection of silicon carbides (SiC, c-SiC_2, c-SiC_3, and SiC_4)[33] along with silane (SiH_4)[34] and methylsilane (CH_3SiH_3)[35] toward IRC+10216 documents a striking gas-phase chemistry, whose initial silicon−carbon bond formation mechanisms are only beginning to emerge.[36] The prospective identification of hydrogenated silicon−carbon clusters such as singlet ethynylsilylene via rotational spectroscopy exploiting the Atacama Large Millimeter/submillimeter Array would exploit circumstellar envelopes as natural laboratories for an exotic silicon−carbon chemistry under extreme conditions. This would provide an opportunity to identify fundamental elementary reactions leading to silicon−carbon bond formation in deep space by guiding astronomical observations with both laboratory experiments under single-collision conditions and theoretical investigations.

METHODS

Experimental Methods. The elementary reaction of dicarbon (C_2; $X^1\Sigma^+_g/a^3\Pi_u$) with silane (SiH_4; X^1A_1) was explored in the gas phase under single-collision conditions in a crossed molecular beams machine.[17] A pulsed molecular beam of dicarbon, prepared via photodissociation of tetrachloroethylene (C_2Cl_4, Sigma-Aldrich, 99.9%) at 248 nm seeded in helium (99.9999%; AirGas) at levels of 1.4% at 300 K, passed through a stainless-steel skimmer. A four-slot chopper wheel was then used to select well-defined speed ratio (S) and peak velocity (v_p) of the dicarbon beam (Table S1), which was then crossed with a pulsed silane beam (99.9997%; Linde) in the interaction region of the scattering chamber. This resulted in a collision energy (E_{col}) of 22.0 ± 0.3 kJ mol^{-1} and a center-of-mass (CM) angle of 35.5 ± 0.4°. After electron-impact ionization of the reactively scattered products, a triply differentially pumped quadrupole mass spectrometer (QMS) using the time-of-flight (TOF) mode was exploited to select ions with a specific mass-to-charge ratio (m/z); these ions were then accelerated toward a stainless-steel target coated with a thin layer of aluminum. This triggered an electron cascade, which utilized an organic scintillator to generate a photon pulse; the latter was then detected by a photomultiplier tube (PMT). The product angular distribution in the laboratory frame (LAB) was obtained by integrating and normalizing the time-of-flight spectra. A forward-convolution routine was then used to convert data from the LAB frame to the CM frame by choosing a product translational energy distribution ($P(E_T)$) and angular distribution ($T(\theta)$) in the CM frame that reproduced the TOF spectra and angular distribution in the LAB frame.

Theoretical Methods. The reactant, intermediate, and product structures were obtained via geometry optimization using the ωB97M-V[37] density functional along with the def2-tzvpd basis set.[38,39] Frequency calculations confirmed no imaginary frequencies for all structures. A transition-state search starting from a guess obtained via the freezing string method was used to obtain transition-state structures, once again using the ωB97M-V functional along with the def2-tzvpd basis set. Frequency calculations confirmed a single imaginary frequency for each transition-state structure. Single-point scaled third-order Møller−Plesset theory using DFT orbitals (sMP3:ωB97M-V)[40] and coupled cluster theory with single, double, and perturbative triple excitations (CCSD(T))[41] were then performed on all structures using the aug-cc-pVXZ family of basis sets[42−44] to obtain high-accuracy energies in the complete basis set limit. Frozen core (FC) corrections were computed using the aug-cc-pCVTZ family of basis sets.[45] The final energies are computed using the formula

$$\begin{aligned} E_{CBS} = {} & E(\text{HF:}\omega\text{B97M-V/aug-cc-pV5Z}) \\ & + E^{corr}(\text{sMP3:}\omega\text{B97M-V/CBS}_{3,4}) \\ & + E(\text{CCSD(T):aug-cc-pVTZ}) \\ & - E(s\text{MP3:}\omega\text{B97M-V/aug-cc-pVTZ}) \\ & + E^{ZPE}(\omega\text{B97M-V/aug-cc-pVTZ}) \end{aligned}$$

where the complete basis set extrapolation for MP3:ωB97M-V is given by

$$\begin{aligned} & E^{corr}(\text{MP3:}\omega\text{B97M-V/CBS}_{3,4}) \\ & = [-27E^{corr}(\text{sMP3:}\omega\text{B97M-V/aug-cc-pVTZ}) \\ & \quad + 64E^{corr}(\text{sMP3:}\omega\text{B97M-V/aug-cc-pVQZ})]/(64-27) \\ & \quad + E^{corr}(\text{sMP3(no FC):}\omega\text{B97M-V/aug-cc-pCVTZ}) \\ & \quad - E^{corr}(\text{sMP3:}\omega\text{B97M-V/aug-cc-pCVTZ}) \end{aligned}$$

The energy of the C_2 molecule was computed by calculating the computationally simpler triplet state, then correcting with an experimental singlet−triplet gap (8.57 kJ mol^{-1}).[46]

QCT trajectories were run starting from the transition-state geometries, as the intermediate structures are too long-lived to study via ab initio molecular dynamics. Only the **i1** → **p3**, **i4** → **p1**, and **i4** → **p2** transition states were considered, as these accounted for the vast majority of products according to RRKM theory. Excess energy at each geometry was distributed randomly among the real modes of the transition states. 200 trajectories for each transition state were run for 240 fs, in which time all trajectories fell to either intermediates or products. All trajectories were run with the ωB97X-D3 functional[47] and the def2-sv(p) basis set. All computations were run with the Q-Chem suite of electronic structure programs.[48]

ASSOCIATED CONTENT

Supporting Information

The Supporting Information is available free of charge at https://pubs.acs.org/doi/10.1021/acs.jpclett.1c03036.

https://doi.org/10.1021/acs.jpclett.1c03036
J. Phys. Chem. Lett. 2021, 12, 10768−10776

Computed geometries, computed reaction rate constants, and full PES figures (PDF)
Video of computed trajectory (C_2 insertion) (MP4)
Video of computed trajectory (H abstraction) (MP4)

AUTHOR INFORMATION

Corresponding Authors

Martin Head-Gordon − *Department of Chemistry, University of California, Berkeley, California 94720, United States;* orcid.org/0000-0002-4309-6669; Email: mhg@cchem.berkeley.edu

Ralf I. Kaiser − *Department of Chemistry, University of Hawai'i at Manoa, Honolulu, Hawaii 96822, United States;* orcid.org/0000-0002-7233-7206; Email: ralfk@hawaii.edu

Authors

Adam Rettig − *Department of Chemistry, University of California, Berkeley, California 94720, United States;* orcid.org/0000-0002-6528-9576

Srinivas Doddipatla − *Department of Chemistry, University of Hawai'i at Manoa, Honolulu, Hawaii 96822, United States*

Zhenghai Yang − *Department of Chemistry, University of Hawai'i at Manoa, Honolulu, Hawaii 96822, United States*

Complete contact information is available at: https://pubs.acs.org/10.1021/acs.jpclett.1c03036

Notes

The authors declare no competing financial interest.

ACKNOWLEDGMENTS

The experimental work at the University of Hawaii was supported by the U.S. National Science Foundation (NSF) under Award CHE-1853541. The computations at UC Berkeley were supported by the National Science Foundation Graduate Research Fellowship under Grant No. (DGE 1752814).

REFERENCES

(1) Reisenauer, H. P.; Maier, G.; Riemann, A.; Hoffmann, R. W. Cyclopropenylidene. *Angew. Chem., Int. Ed. Engl.* **1984**, *23* (8), 641−641.

(2) McCarthy, M. C.; Gottlieb, C. A.; Gupta, H.; Thaddeus, P. Laboratory and Astronomical Identification of the Negative Molecular Ion C_6H. *Astrophys. J.* **2006**, *652* (2), L141−L144.

(3) Maier, G.; Reisenauer, H. P.; Schwab, W.; Carsky, P.; Hess, B. A.; Schaad, L. J. Vinylidene Carbene: A New C_3H_2 Species. *J. Am. Chem. Soc.* **1987**, *109* (17), 5183−5188.

(4) Cernicharo, J.; Gottlieb, C. A.; Guelin, M.; Thaddeus, P.; Vrtilek, J. M. Astonomical and Laboratory Detection of the SiC Radical. *Astrophys. J.* **1989**, *341*, L25−L28.

(5) Herges, R.; Mebel, A. Propargylene. *J. Am. Chem. Soc.* **1994**, *116* (18), 8229−8237.

(6) Osborn, D. L.; Vogelhuber, K. M.; Wren, S. W.; Miller, E. M.; Lu, Y.-J.; Case, A. S.; Sheps, L.; McMahon, R. J.; Stanton, J. F.; Harding, L. B.; Ruscic, B.; Lineberger, W. C. Electronic States of the Quasilinear Molecule Propargylene (HCCCH) from Negative Ion Photoelectron Spectroscopy. *J. Am. Chem. Soc.* **2014**, *136* (29), 10361−10372.

(7) Ribeiro, J. M.; Mebel, A. M. Reaction Mechanism and Product Branching Ratios of the CH + C_3H_4 Reactions: A Theoretical Study. *Phys. Chem. Chem. Phys.* **2017**, *19* (22), 14543−14554.

(8) Maksyutenko, P.; Zhang, F.; Gu, X.; Kaiser, R. I. A Crossed Molecular Beam Study on the Reaction of Methylidyne Radicals [$CH(X^2\Pi)$] with Acetylene [$C_2H_2(X^1\Sigma_g^+)$]—Competing C_3H_2 + H and C_3H + H_2 Channels. *Phys. Chem. Chem. Phys.* **2011**, *13* (1), 240−252.

(9) Wilson, A. V.; Parker, D. S. N.; Zhang, F.; Kaiser, R. I. Crossed Beam Study of the Atom-Radical Reaction of Ground State Carbon Atoms ($C(^3P)$) with the Vinyl Radical (C_2H_3 (X^2A')). *Phys. Chem. Chem. Phys.* **2012**, *14* (2), 477−481.

(10) Wu, Q.; Simmonett, A. C.; Yamaguchi, Y.; Li, Q.; Schaefer, H. F. Silacyclopropenylidene and Its Most Important SiC_2H_2 Isomers. *J. Phys. Chem. C* **2010**, *114* (12), 5447−5457.

(11) Maier, G.; Reisenauer, H. P.; Pacl, H. C_2H_2Si Isomers: Generation by Pulsed Flash Pyrolysis and Matrix-Spectroscopic Identification. *Angew. Chem., Int. Ed. Engl.* **1994**, *33* (12), 1248−1250.

(12) Maier, G.; Reisenauer, H. P.; Egenolf, H. Reaction of Silicon Atoms with Acetylene and Ethylene: Generation and Matrix-Spectroscopic Identification of C_2H_2Si and C_2H_4Si Isomers. *Eur. J. Org. Chem.* **1998**, *1998* (7), 1313−1317.

(13) Izuha, M.; Yamamoto, S.; Saito, S. Microwave Spectrum and Molecular Structure of Silacyclopropenylidene c-C_2H_2Si. *Can. J. Phys.* **1994**, *72* (11−12), 1206−1212.

(14) McCarthy, M. C.; Thaddeus, P. The Rotational Spectra of H_2CCSi and H_2C_4Si. *J. Mol. Spectrosc.* **2002**, *211* (2), 228−234.

(15) Sherrill, C. D.; Brandow, C. G.; Allen, W. D.; Schaefer, H. F. Cyclopropyne and Silacyclopropyne: A World of Difference. *J. Am. Chem. Soc.* **1996**, *118* (30), 7158−7163.

(16) Parker, D. S. N.; Wilson, A. V.; Kaiser, R. I.; Mayhall, N. J.; Head-Gordon, M.; Tielens, A. G. G. M. On the Formation of Silacyclopropenylidene (c-SiC_2H_2) and Its Role in the Organosilicon Chemistry in the Interstellar Medium. *Astrophys. J.* **2013**, *770* (1), 33.

(17) Guo, Y.; Gu, X.; Kawamura, E.; Kaiser, R. I. Design of a Modular and Versatile Interlock System for Ultrahigh Vacuum Machines: A Crossed Molecular Beam Setup as a Case Study. *Rev. Sci. Instrum.* **2006**, *77* (3), 034701.

(18) Thomas, A. M.; Lucas, M.; Zhao, L.; Liddiard, J.; Kaiser, R. I.; Mebel, A. M. A Combined Crossed Molecular Beams and Computational Study on the Formation of Distinct Resonantly Stabilized C_5H_3 Radicals *via* Chemically Activated C_5H_4 and C_6H_6 Intermediates. *Phys. Chem. Chem. Phys.* **2018**, *20* (16), 10906−10925.

(19) Kaiser, R. I.; Maksyutenko, P.; Ennis, C.; Zhang, F.; Gu, X.; Krishtal, S. P.; Mebel, A. M.; Kostko, O.; Ahmed, M. Untangling the Chemical Evolution of Titan's Atmosphere and Surface-from Homogeneous to Heterogeneous Chemistry. *Faraday Discuss.* **2010**, *147* (0), 429−478.

(20) Yang, T.; Bertels, L.; Dangi, B. B.; Li, X.; Head-Gordon, M.; Kaiser, R. I. Gas Phase Formation of c-SiC_3 Molecules in the Circumstellar Envelope of Carbon Stars. *Proc. Natl. Acad. Sci. U. S. A.* **2019**, *116* (29), 14471−14478.

(21) Kaiser, R. I.; Krishtal, S. P.; Mebel, A. M.; Kostko, O.; Ahmed, M. An Experimental and Theoretical Study of the Ionization Energies of SiC_2H_x (x = 0, 1, 2) Isomers. *Astrophys. J.* **2012**, *761* (2), 178.

(22) Talbi, D. An Extensive Ab Initio Study of the Si + C_2H_2 and Si + C_2H_4 Reactions in Relation to the Silicon Astrochemistry. *Chem. Phys.* **2005**, *313* (1−3), 17−23.

(23) Wu, Q.; Hao, Q.; Wilke, J. J.; Simmonett, A. C.; Yamaguchi, Y.; Li, Q.; Fang, D.-C.; Schaefer, H. F. Anharmonic Vibrational Analyses for the 1-Silacyclopropenylidene Molecule and Its Three Isomers. *Mol. Phys.* **2012**, *110* (9−10), 783−800.

(24) Takahashi, M.; Sakamoto, K. Ab Initio Study of the Photochemistry of c-C_2H_2Si. *J. Phys. Chem. A* **2004**, *108* (35), 7301−7305.

(25) Thorwirth, S.; Harding, M. E. Coupled-Cluster Calculations of C_2H_2Si and CNHSi Structural Isomers. *J. Chem. Phys.* **2009**, *130* (21), 214303.

(26) Kassaee, M. Z.; Musavi, S. M.; Buazar, F.; Ghambarian, M. Ab Initio Study of Singlet-Triplet Energy Separations in C_2HXSi Silylenes (X = H, F, Cl and Br). *J. Mol. Struct.: THEOCHEM* **2005**, *722* (1−3), 151−160.

(27) Kaiser, R. I.; Chiong, C. C.; Asvany, O.; Lee, Y. T.; Stahl, F.; von R. Schleyer, P.; Schaefer, H. F. Chemical Dynamics of D1-Methyldiacetylene (CH_3CCCCD; X^1A_1) and D1-Ethynylallene

($H_2CCCH(C_2D)$; X^1A') Formation from Reaction of $C_2D(X^2\Sigma^+)$ with Methylacetylene, CH_3 $CCH(X^1A_1)$. *J. Chem. Phys.* **2001**, *114* (8), 3488−3496.
(28) Luke, B. T.; Pople, J. A.; Krogh-Jespersen, M. B.; Apeloig, Y.; Karni, M.; Chandrasekhar, J.; von Ragué Schleyer, P. A Theoretical Survey of Unsaturated or Multiply Bonded and Divalent Silicon Compounds. Comparison with Carbon Analogues. *J. Am. Chem. Soc.* **1986**, *108* (2), 270−284.
(29) Walsh, R. Bond Dissociation Energy Values in Silicon-Containing Compounds and Some of Their Implications. *Acc. Chem. Res.* **1981**, *14* (8), 246−252.
(30) Doncaster, A. M.; Walsh, R. Kinetics of the Gas-Phase Reaction between Iodine and Monosilane and the Bond Dissociation Energy $D(H_3Si-H)$. *Int. J. Chem. Kinet.* **1981**, *13* (5), 503−514.
(31) Seburg, R. A.; Patterson, E. V.; Stanton, J. F.; McMahon, R. J. Structures, Automerizations, and Isomerizations of C_3H_2 Isomers. *J. Am. Chem. Soc.* **1997**, *119* (25), 5847−5856.
(32) Horner, D. A.; Curtiss, L. A.; Gruen, D. M. A Theoretical Study of the Energetics of Insertion of Dicarbon (C_2) and Vinylidene into Methane CH Bonds. *Chem. Phys. Lett.* **1995**, *233* (3), 243−248.
(33) Thaddeus, P.; Cummins, S. E.; Linke, R. A. Identification of the SiCC Radical toward IC + 10216 - The First Molecular Ring in an Astronomical Source. *Astrophys. J.* **1984**, *283*, L45.
(34) Goldhaber, D. M.; Betz, A. L. Silane in IRC + 10216. *Astrophys. J.* **1984**, *279*, L55−L58.
(35) Cernicharo, J.; McCarthy, M. C.; Gottlieb, C. A.; Agúndez, M.; Prieto, L. V.; Baraban, J. H.; Changala, P. B.; Guélin, M.; Kahane, C.; Martin-Drumel, M. A.; Patel, N. A.; Reilly, N. J.; Stanton, J. F.; Quintana-Lacaci, G.; Thorwirth, S.; Young, K. H. Discovery of SiCSi in IRC+10216: A Missing Link between Gas and Dust Carriers of Si-C Bonds. *Astrophys. J., Lett.* **2015**, *806* (1), L3.
(36) Yang, Z.; Doddipatla, S.; Kaiser, R. I.; Nikolayev, A. A.; Azyazov, V. N.; Mebel, A. M. On the Synthesis of the Astronomically Elusive 1-Ethynyl-3-Silacyclopropenylidene ($c\text{-}SiC_4H_2$) Molecule in Circumstellar Envelopes of Carbon-Rich Asymptotic Giant Branch Stars and Its Potential Role in the Formation of the Silicon Tetracarbide Chain (SiC_4). *Astrophys. J., Lett.* **2021**, *908* (2), L40.
(37) Mardirossian, N.; Head-Gordon, M. ωB97M-V: A Combinatorially Optimized, Range-Separated Hybrid, Meta-GGA Density Functional with VV10 Nonlocal Correlation. *J. Chem. Phys.* **2016**, *144* (21), 214110.
(38) Weigend, F.; Ahlrichs, R. Balanced Basis Sets of Split Valence, Triple Zeta Valence and Quadruple Zeta Valence Quality for H to Rn: Design and Assessment of Accuracy. *Phys. Chem. Chem. Phys.* **2005**, *7* (18), 3297.
(39) Rappoport, D.; Furche, F. Property-Optimized Gaussian Basis Sets for Molecular Response Calculations. *J. Chem. Phys.* **2010**, *133* (13), 134105.
(40) Rettig, A.; Hait, D.; Bertels, L. W.; Head-Gordon, M. Third-Order Møller-Plesset Theory Made More Useful? The Role of Density Functional Theory Orbitals. *J. Chem. Theory Comput.* **2020**, *16* (12), 7473−7489.
(41) Raghavachari, K.; Trucks, G. W.; Pople, J. A.; Head-Gordon, M. A Fifth-Order Perturbation Comparison of Electron Correlation Theories. *Chem. Phys. Lett.* **1989**, *157* (6), 479−483.
(42) Dunning, T. H. Gaussian Basis Sets for Use in Correlated Molecular Calculations. I. The Atoms Boron through Neon and Hydrogen. *J. Chem. Phys.* **1989**, *90* (2), 1007−1023.
(43) Kendall, R. A.; Dunning, T. H.; Harrison, R. J. Electron Affinities of the First-Row Atoms Revisited. Systematic Basis Sets and Wave Functions. *J. Chem. Phys.* **1992**, *96* (9), 6796−6806.
(44) Woon, D. E.; Dunning, T. H. Gaussian Basis Sets for Use in Correlated Molecular Calculations. III. The Atoms Aluminum through Argon. *J. Chem. Phys.* **1993**, *98* (2), 1358−1371.
(45) Woon, D. E.; Dunning, T. H. Gaussian Basis Sets for Use in Correlated Molecular Calculations. V. Core-valence Basis Sets for Boron through Neon. *J. Chem. Phys.* **1995**, *103* (11), 4572.
(46) Gurvich, L. V.; Veyts, I. V.; Alcock, C. B. *Thermodynamic Properties of Individual Substances*, 4th ed.; Begell House, 1994.
(47) Lin, Y.-S.; Li, G.-D.; Mao, S.-P.; Chai, J.-D. Long-Range Corrected Hybrid Density Functionals with Improved Dispersion Corrections. *J. Chem. Theory Comput.* **2013**, *9* (1), 263−272.
(48) Epifanovsky, E.; Gilbert, A. T. B.; Feng, X.; Lee, J.; Mao, Y.; Mardirossian, N.; Pokhilko, P.; White, A. F.; Coons, M. P.; Dempwolff, A. L.; Gan, Z.; Hait, D.; Horn, P. R.; Jacobson, L. D.; Kaliman, I.; Kussmann, J.; Lange, A. W.; Lao, K. U.; Levine, D. S.; Liu, J.; McKenzie, S. C.; Morrison, A. F.; Nanda, K. D.; Plasser, F.; Rehn, D. R.; Vidal, M. L.; You, Z.-Q.; Zhu, Y.; Alam, B.; Albrecht, B. J.; Aldossary, A.; Alguire, E.; Andersen, J. H.; Athavale, V.; Barton, D.; Begam, K.; Behn, A.; Bellonzi, N.; Bernard, Y. A.; Berquist, E. J.; Burton, H. G. A.; Carreras, A.; Carter-Fenk, K.; Chakraborty, R.; Chien, A. D.; Closser, K. D.; Cofer-Shabica, V.; Dasgupta, S.; de Wergifosse, M.; Deng, J.; Diedenhofen, M.; Do, H.; Ehlert, S.; Fang, P.-T.; Fatehi, S.; Feng, Q.; Friedhoff, T.; Gayvert, J.; Ge, Q.; Gidofalvi, G.; Goldey, M.; Gomes, J.; González-Espinoza, C. E.; Gulania, S.; Gunina, A. O.; Hanson-Heine, M. W. D.; Harbach, P. H. P.; Hauser, A.; Herbst, M. F.; Hernández Vera, M.; Hodecker, M.; Holden, Z. C.; Houck, S.; Huang, X.; Hui, K.; Huynh, B. C.; Ivanov, M.; Jász, Á.; Ji, H.; Jiang, H.; Kaduk, B.; Kähler, S.; Khistyaev, K.; Kim, J.; Kis, G.; Klunzinger, P.; Koczor-Benda, Z.; Koh, J. H.; Kosenkov, D.; Koulias, L.; Kowalczyk, T.; Krauter, C. M.; Kue, K.; Kunitsa, A.; Kus, T.; Ladjánszki, I.; Landau, A.; Lawler, K. V.; Lefrancois, D.; Lehtola, S.; Li, R. R.; Li, Y.-P.; Liang, J.; Liebenthal, M.; Lin, H.-H.; Lin, Y.-S.; Liu, F.; Liu, K.-Y.; Loipersberger, M.; Luenser, A.; Manjanath, A.; Manohar, P.; Mansoor, E.; Manzer, S. F.; Mao, S.-P.; Marenich, A. V.; Markovich, T.; Mason, S.; Maurer, S. A.; McLaughlin, P. F.; Menger, M. F. S. J.; Mewes, J.-M.; Mewes, S. A.; Morgante, P.; Mullinax, J. W.; Oosterbaan, K. J.; Paran, G.; Paul, A. C.; Paul, S. K.; Pavošević, F.; Pei, Z.; Prager, S.; Proynov, E. I.; Rák, Á.; Ramos-Cordoba, E.; Rana, B.; Rask, A. E.; Rettig, A.; Richard, R. M.; Rob, F.; Rossomme, E.; Scheele, T.; Scheurer, M.; Schneider, M.; Sergueev, N.; Sharada, S. M.; Skomorowski, W.; Small, D. W.; Stein, C. J.; Su, Y.-C.; Sundstrom, E. J.; Tao, Z.; Thirman, J.; Tornai, G. J.; Tsuchimochi, T.; Tubman, N. M.; Veccham, S. P.; Vydrov, O.; Wenzel, J.; Witte, J.; Yamada, A.; Yao, K.; Yeganeh, S.; Yost, S. R.; Zech, A.; Zhang, I. Y.; Zhang, X.; Zhang, Y.; Zuev, D.; Aspuru-Guzik, A.; Bell, A. T.; Besley, N. A.; Bravaya, K. B.; Brooks, B. R.; Casanova, D.; Chai, J.-D.; Coriani, S.; Cramer, C. J.; Cserey, G.; DePrince, A. E.; DiStasio, R. A.; Dreuw, A.; Dunietz, B. D.; Furlani, T. R.; Goddard, W. A.; Hammes-Schiffer, S.; Head-Gordon, T.; Hehre, W. J.; Hsu, C.-P.; Jagau, T.-C.; Jung, Y.; Klamt, A.; Kong, J.; Lambrecht, D. S.; Liang, W.; Mayhall, N. J.; McCurdy, C. W.; Neaton, J. B.; Ochsenfeld, C.; Parkhill, J. A.; Peverati, R.; Rassolov, V. A.; Shao, Y.; Slipchenko, L. V.; Stauch, T.; Steele, R. P.; Subotnik, J. E.; Thom, A. J. W.; Tkatchenko, A.; Truhlar, D. G.; Van Voorhis, T.; Wesolowski, T. A.; Whaley, K. B.; Woodcock, H. L.; Zimmerman, P. M.; Faraji, S.; Gill, P. M. W.; Head-Gordon, M.; Herbert, J. M.; Krylov, A. I. Software for the Frontiers of Quantum Chemistry: An Overview of Developments in the Q-Chem 5 Package. *J. Chem. Phys.* **2021**, *155* (8), 084801.

https://doi.org/10.1021/acs.jpclett.1c03036
J. Phys. Chem. Lett. 2021, 12, 10768−10776